

# Preparation, characterization, antimicrobial and anticancer activities of Schiff base mixed ligand complexes

H. F. Abd El-Halim<sup>1</sup> · M. M. Omar<sup>2</sup> · Mahmoud N. Anwar<sup>3</sup>

Received: 20 October 2016 / Accepted: 22 May 2017 / Published online: 3 June 2017  
© Akadémiai Kiadó, Budapest, Hungary 2017

**Abstract** A new Schiff base ligand (HL) derived from quinoline-2-carboxaldehyde with 2-aminophenol (1:1 molar ratio) and its mixed ligand complexes, viz. 2,2'-bipyridine (1:1:1 molar ratio), have been synthesized and characterized by elemental analysis, spectroscopic studies, X-ray diffraction, ESR, magnetic and thermal analysis. The molar conductance measurement of mixed ligand complexes in DMF showed that Zn(II) and Cd(II) complexes were nonelectrolytes; however, Cr(III), Mn(II), Fe(III), Co(II), Ni(II) and Cu(II) complexes were electrolytes. The transition metal complexes had octahedral geometry with a general molecular formulae  $[M(L)(2,2'\text{-bipy})(H_2O)]Cl_x \cdot nH_2O$  ( $M = Cr(III)$  ( $x = n = 2$ ),  $Mn(II)$  and  $Co(II)$  ( $x = 1$ ,  $n = 0$ ),  $Ni(II)$  and  $Cu(II)$  ( $x = n = 1$ ) and  $[M(L)(2,2'\text{-bipy})Cl]Cl_x \cdot nH_2O$  ( $M = Fe(III)$  ( $x = 1$ ,  $n = 3$ ),  $Zn(II)$  ( $x = 0$ ,  $n = 1$ ) and  $Cd(II)$  ( $x = 0$ ,  $n = 2$ )). Also, Schiff base ligand and its mixed ligand complexes were screened against Gram-positive bacteria (*Streptococcus pneumoniae*, *Bacillus subtilis*), Gram-negative bacteria (*Pseudomonas aeruginosa*, *Escherichia coli*) and fungal species (*Aspergillus fumigatus*, *Candida albicans*). Gentamicin, ampicillin and amphotericin B were used as standard drugs for Gram positive, Gram negative and antifungal activity,

respectively. The results showed that all mixed ligand complexes have antimicrobial activity higher than free Schiff base ligand. In addition, anticancer activity of Schiff base ligand and its mixed ligand metal complexes were also tested against breast cancer cell line (MCF-7) and colon cancer cell line (HCT-116). Cd(II) complex showed the highest  $IC_{50}$  against two cell lines.

**Keywords** Mixed ligand complexes · Schiff base · Quinoline · (2,2'-Bipy) · Antibacterial activity · Anticancer activity

## Introduction

Mixed ligand complexes of Schiff base which have nitrogen, oxygen and sulfur donor atoms in their backbones play an important role in biological process as exemplified by many instances in which enzymes were known to be activated by metal ions [1–3]. Among mixed ligand complexes derived from quinoline and quinoline derivative [4–6], quinolinones are the most important class of heterocyclic compounds and a part of the alkaloid family [7]. Quinolines have emerged as potential therapeutic agents because of their conformational rigidity and improved physical properties, such as charge density or lipophilicity, and pharmacological advantages such as metabolic stability and oral bioavailability [7, 8]. Quinolines, considered as the backbone for most natural products, were used for the design of many synthetic compounds having diverse pharmacological applications such as antibacterial, antifungal [9, 10], anticancer [11], antimalarial and antiviral [12], antiproliferative [13], antiplasmodial [14], anti-inflammatory [15], anticonvulsant, antihypertensive [16], analgesic, vasorelaxing [17], immunosuppressive [18], and as a basis of development of many medicinal drugs used

**Electronic supplementary material** The online version of this article (doi:10.1007/s10973-017-6491-1) contains supplementary material, which is available to authorized users.

✉ H. F. Abd El-Halim  
Hanan.Farouk2@yahoo.com

<sup>1</sup> Pharmaceutical Chemistry Department, Faculty of Pharmacy, Misr International University, Cairo, Egypt

<sup>2</sup> Chemistry Department, Faculty of Science, Cairo University, Giza, Egypt

<sup>3</sup> El-Nasr Co. for Intermediate Chemicals (NCIC), Giza, Egypt

as potential application as DNA-targeted chemotherapeutics [19] and antioxidant [20]. In chemistry, quinolines can be used as corrosion inhibitor [21], detector [22], catalytic activity [23] and sensor [24].

In the present work, a new Schiff base (HL) ligand derived from the condensation of quinoline-2-carboxaldehyde with 2-aminophenol and its mixed ligand complexes, viz. 2,2'-bipyridine with a series of transition metal ions of Cr(III), Mn(II), Fe(III), Co(II), Ni(II), Cu(II), Zn(II) and Cd(II), have been synthesized. The Schiff base ligand and its mixed ligand complexes were characterized by using elemental analysis, IR spectra, <sup>1</sup>H-NMR, mass spectrum, UV-visible analysis, conductivity measurement, magnetic behavior and electronic spectra, solid reflectance, ESR, thermal analysis and X-ray diffraction. The antimicrobial activities of Schiff base ligand and the mixed ligand complexes were tested. In addition, anticancer activity of Schiff base ligand and its mixed ligand metal complexes were tested against breast cancer cell line (MCF-7) and colon cancer cell line (HCT-116).

## Experimental

### Materials

All chemicals were purchased and used without further purification. Quinoline-2-carboxaldehyde, 2-aminophenol and 2,2'-bipyridine were supplied from Arcos organic—USA, Combrain chemical and Fluka Chemie, respectively. Metal chloride salts including CrCl<sub>3</sub>·6H<sub>2</sub>O, MnCl<sub>2</sub>·2H<sub>2</sub>O (Sigma), FeCl<sub>3</sub>·6H<sub>2</sub>O (Prolabo), CoCl<sub>2</sub>·6H<sub>2</sub>O, NiCl<sub>2</sub>·6H<sub>2</sub>O, CuCl<sub>2</sub>·2H<sub>2</sub>O, ZnCl<sub>2</sub>·2H<sub>2</sub>O and CdCl<sub>2</sub> (BDH) were also used. Dimethylformamide (DMF) 97% and ethanol (99%, 95%) (Adwic) have been used as organic solvents.

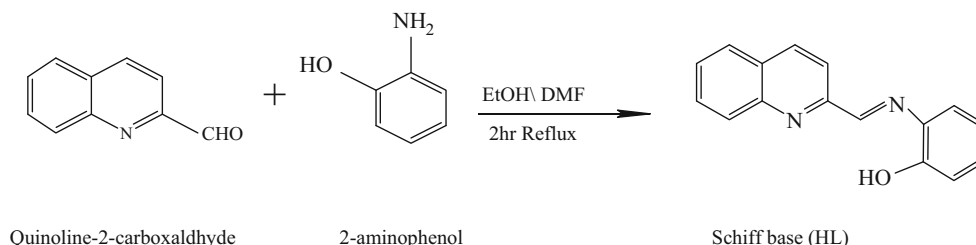
### Physical measurements and analytical techniques

Microanalysis of carbon, hydrogen and nitrogen was carried out at the Microanalytical Center, Cairo University, Egypt, using CHNS-932 (LECO) Vario Elemental Analyzer. Metal ions have been determined by titration against standard

EDTA solution [25–27]. FT-IR spectra were recorded on a Perkin-Elmer 1650 spectrometer 4000–400 cm<sup>-1</sup> in KBr pellets. <sup>1</sup>H-NMR spectra, as a solution in DMSO-*d*<sub>6</sub>, were recorded on Varian-Oxford Mercury 300 MHz “NMR 300” at room temperature using TMS as an internal standard. Mass spectra were carried out by the EI technique at 70 eV using MS-5988 GS-MS Hewlett–Packard instrument at the Microanalytical Center, National Center for Research, Egypt. Molar conductivities of 10<sup>-3</sup> M solutions of the solid complexes in DMF were measured using Jenway 4010 conductivity meter. Melting points were measured by Stuart melting point—SMP 30 UK. The molar magnetic susceptibility was measured on powdered samples using the Faraday method, the diamagnetic corrections were made by Pascal's constant, and Hg[Co(SCN)<sub>4</sub>] was used as a calibrant. UV-visible spectra were carried out on UV mini-1240, UV-Vis spectrophotometer Shimadzu. The thermogravimetric analysis (TG and DTG) of the solid complexes was carried out using Shimadzu TGA-50H thermal analyzer, flow rate of 10 °C min<sup>-1</sup> atmosphere and nitrogen with flow rate of 20 mL min<sup>-1</sup>, from 25 to 1000 °C. The X-ray powder diffraction analyses were carried out using Philips Analytical X-ray BV, diffractometer type PW 1840. Radiation was provided by copper target (Cu anode 2000 W) high-intensity X-ray tube operated at 40 kV and 30 mA. Divergence and the receiving slits were 1 and 0.15 mm, respectively. Electron spin resonance spectra were also recorded by JES-FE2XG ESR spectrophotometer at atomic energy commission. Antibacterial, antifungal and anticancer activities were carried out at the Regional Center for Mycology and Biotechnology, AL-Azhar University, Egypt.

### Synthesis of Schiff base ligand (HL)

Quinoline-2-carboxaldehyde (2.5 g, 3.18 mmol) dissolved in 50 mL of DMF was added to 2-aminophenol (1.59 g, 3.18 mmol) and dissolved in 50 mL of ethanol, in a molar ratio 1:1. The mixture was refluxed for 2 h. A dark brown solid was precipitated, filtered, washed with ethanol and weighed. The yield was 79%. Scheme 1 shows the general reaction of synthesis and structure of Schiff base ligand.



**Scheme 1** The general reaction for the synthesis of Schiff base ligand (HL)

## Synthesis of mixed ligand metal complexes

An ethanolic solution of metal chloride of Cr(III), Mn(II), Fe(III), Co(II), Ni(II), Cu(II), Zn(II) and Cd(II) (0.374, 0.227, 0.379, 0.335, 0.239, 0.242 and 0.334, 0.306 g (1.4 mmol)) was added to a mixture of (0.35 g, 1.4 mmol) Schiff base ligand, HL dissolved in 50 mL DMF and (0.225 g, 1.4 mmol) of 2,2'-bipyridine dissolved in 20 mL of EtOH, in a molar ratio 1:1:1. The mixture was refluxed for 2 h. The solid precipitates of metal complexes were filtered and washed with small portion of ethanol, then air-dried and weighed. The percent yield of mixed ligand complexes is mentioned in Table 1. The general reaction for synthesis of mixed ligand complexes and their general structure is represented in Scheme 2.

## Biological testing

### Antibacterial and antifungal

Antimicrobial tests were carried out using the agar well-diffusion method [28]. The free Schiff base ligand (HL) and the mixed ligand complexes were tested in vitro for their antibacterial activity against the Gram-positive bacteria (*Streptococcus pneumoniae* (RCMB010010), *Bacillus subtilis* (RCMB 010067)) and Gram-negative bacteria (*Pseudomonas aeruginosa* (RCMB 010043), *Escherichia coli* (RCMB 010052)). Antifungal activity was carried out against *Aspergillus fumigatus* (RCMB 02568) and *Candida albicans* (RCMB 05036) using Sabouraud dextrose agar medium. Gentamicin, ampicillin and amphotericin B were used as standard drugs for Gram positive, Gram negative and antifungal activity, respectively. DMSO was used as solvent control. The compounds were tested at a concentration of (5 mg mL<sup>-1</sup>) against both bacterial and fungal strains. The sterilized media were poured onto the sterilized petri dishes (20 mL, each petri dish) and allowed to solidify. Wells of 6 mm diameter were made in the solidified media with the help of sterile borer. A sterile swab was used to evenly distribute microbial suspension over the surface of solidified media and solution, and the tested samples were added to each well with the help of micropipette. The plates were incubated at 37 °C for 24 h in case of antimicrobial activity and at 25 °C for 48 h for antifungal activity. These tests were carried out in triplicate, and zone of inhibition was measured in mm scale.

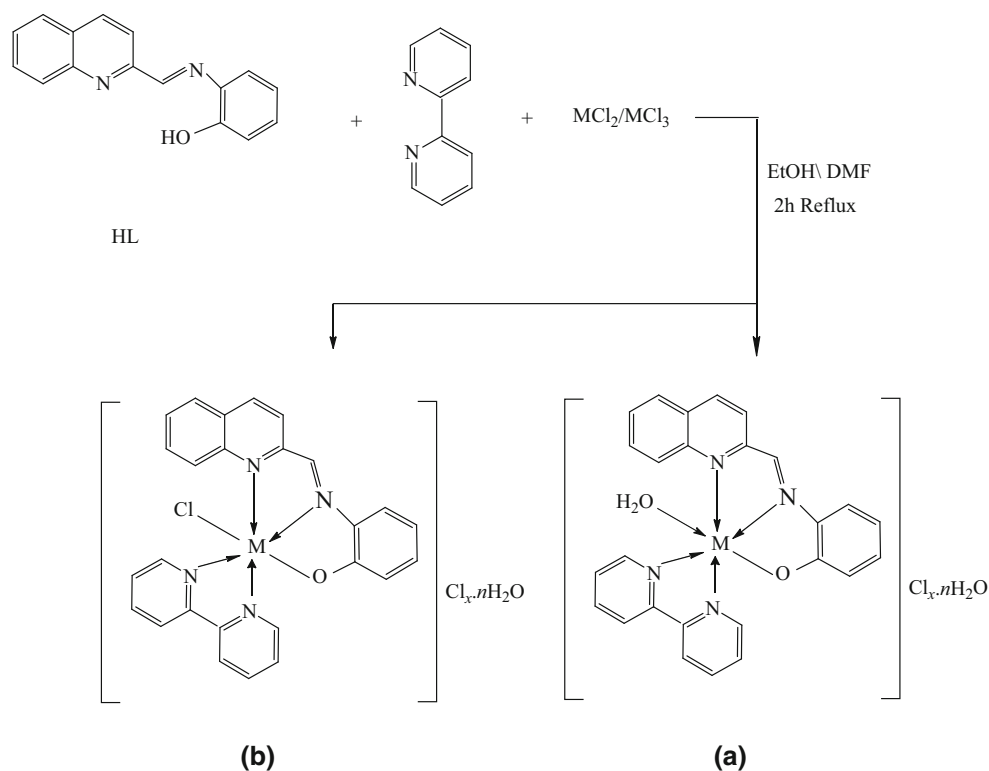
### Anticancer activity

The cytotoxicity evaluation was carried out using viability assay. The free Schiff base ligand and its mixed ligand complexes were tested against breast cell line (MCF-7) and colon cell line (HCT-116). The cells were propagated in

**Table 1** Analytical and physical data for Schiff base ligand (HL) and its mixed ligand complexes

Compound	Color/%yield	MP/°C	$\Delta m/\Omega^{-1} \text{ mol}^{-1} \text{ cm}^2$	$\mu_{\text{eff}}/\text{B.M.}$	Found/calcd. %			
					C	H	N	M
HL	Brown/79%	197	—	—	77.53/77.42	4.54/4.83	11.70/11.29	—
[Cr(L)(2,2'-bipy)(H <sub>2</sub> O)]Cl <sub>2</sub> ·2H <sub>2</sub> O	Dark brown/91%	280	109.3	4.47	53.93/53.79	4.22/4.31	9.57/9.66	8.50/8.96
[Mn(L)(2,2'-bipy)(H <sub>2</sub> O)]Cl	Brown/87%	>380	53.70	5.72	61.22/61.12	4.82/4.11	10.89/10.97	10.72/10.58
[Fe(L)(2,2'-bipy)Cl]Cl·3H <sub>2</sub> O	Violet/84%	230	67.70	5.38	53.40/53.42	4.47/4.28	9.50/9.59	9.98/9.60
[Co(L)(2,2'-bipy)(H <sub>2</sub> O)]Cl	Black/88%	380	60.70	5.44	60.93/60.52	4.22/4.10	10.52/10.86	11.52/11.48
[Ni(L)(2,2'-bipy)(H <sub>2</sub> O)]Cl·H <sub>2</sub> O	Black/93%	>380	88.70	3.13	58.93/58.26	4.66/4.30	10.30/10.46	11.30/11.39
[Cu(L)(2,2'-bipy)(H <sub>2</sub> O)]Cl·H <sub>2</sub> O	Black/98%	227	78.60	1.92	58.22/58.04	4.35/4.28	10.96/10.42	11.71/11.72
[Zn(L)(2,2'-bipy)Cl]·H <sub>2</sub> O	Black/97%	232	15.70	Diamagnetic	59.36/59.83	4.36/4.03	9.93/10.74	12.10/12.47
[Cd(L)(2,2'-bipy)Cl]·2H <sub>2</sub> O	Brown/90%	>380	10.00	Diamagnetic	53.52/53.19	3.56/3.92	9.01/9.55	19.47/19.10

**Scheme 2** Synthesis of mixed ligand metal complexes of Schiff base (HL) with (2,2'-Bipy), **a**  $M = Cr(III)$  ( $x = n = 2$ ),  $Mn(II)$  and  $Co(II)$  ( $x = 1, n = 0$ ),  $Ni(II)$  and  $Cu(II)$  ( $x = n = 1$ ) and **b**  $M = Fe(III)$  ( $x = 1, n = 3$ ),  $Zn(II)$  ( $x = 0, n = 1$ ),  $Cd(II)$  ( $x = 0, n = 2$ )



Dulbecco's modified Eagle's medium (DMEM) supplemented with 10% heated-inactivated fetal bovine serum, 1% L-glutamine, HEPES buffer and  $50 \mu\text{g mL}^{-1}$  gentamycin. All cells maintained at  $37^\circ\text{C}$  in a humidified atmosphere with 5%  $\text{CO}_2$  and were subcultured two times a week. For cytotoxicity assay, the cells were seeded in 96-well plate at a cell concentration of  $1 \times 10^4$  cells per well in  $100 \mu\text{L}$  of growth medium. Fresh medium containing different concentration of the tested sample was added after 24 h of seeding. Serial twofold dilution of the tested chemical compound was added to confluent cell monolayers into 96-well, flat-bottomed microtiter plates (Falcon, NJ, USA) using a multichannel pipette. The microtiter plates were incubated at  $37^\circ\text{C}$  in a humidified incubator with 5%  $\text{CO}_2$  for a period of 48 h. Three wells were used for each concentration of the test sample. Control cells were incubated without test sample and without DMSO. The little percentage of DMSO present in the wells (maximal 0.1%) was found not to affect the experiment. After incubation of wells for 24 h at  $37^\circ\text{C}$ , various concentrations of sample (50, 25, 12.5, 6.25, 3.125 and  $1.56 \mu\text{g}$ ) were added, and the incubation was continued for 48 h and viable cells yield was determined by a colorimetric method. The 50% inhibitory concentration ( $\text{IC}_{50}$ ), the concentration required to causes toxic effects in 50% of the cells, was estimated from graphic plots. In brief, after the end of the incubation period, media were aspirated and the crystal violet solution (1%) was added to each well

for at least 30 min. The stain was removed and the plates were rinsed using tap water until all excess stain is removed. Glacial acetic acid (30%) was then added to all wells and mixed thoroughly, and then, absorbance of the plates was measured after gently shaken on Microplate reader (TECAN, Inc), using a test wavelength of 490 nm. All results were corrected for background absorbance detected in wells without added stain. Treated samples were compared with the cell control in the absence of the tested compounds. All experiments were carried out in triplicate. The cell cytotoxic effect of each tested compound was calculated [29].

## Results and discussion

### Elemental analyses

The results of elemental analyses with suggested molecular formula and physical properties of Schiff base ligand and its mixed ligand complexes are shown in Table 1. The Schiff base and its mixed ligand complexes were insoluble in most common organic solvents except DMF and DMSO.

### Molar conductance measurements

The molar conductance values of the synthesized complexes obtained in DMF as a solvent with ( $1 \times 10^{-3} \text{ M}$ )

concentration at room temperature are listed in Table 1. The low molar conductance values of Zn(II) and Cd(II) complexes showed non-electrolytic nature. However, the molar conductance values of Cr(III), Mn(II), Fe(III), Co(II), Ni(II) and Cu(II) complexes showed that these chelates were ionic in nature.

### UV-Vis studies

Absorption spectral data of the free Schiff base ligand (HL) and its mixed ligand complexes were carried out in DMF. UV-Vis spectra were recorded for these complexes with ( $1 \times 10^{-4}$  M) solutions in the range of 200–700 nm. A band at 267 nm may be attributed to  $\pi-\pi^*$  transition of the aromatic ring. The second band observed at 310 nm can be attributed to  $n-\pi^*$  electronic transition of azomethine group in the free Schiff base ligand [30]. In the spectra of the mixed ligand complexes, the two bands were shifted to higher frequencies (bathochromic shift) where the  $\pi-\pi^*$  and  $n-\pi^*$  transition bands were observed at 269–282 and 315–351 nm, respectively, due to the metals chelation (Supplementary Table 2). The spectra of Cr(III), Mn(II), Fe(III), Co(II), Ni(II), Cu(II), Zn(II) and Cd(II) complexes showed absorption bands at 440, 481, 425, 420, 510, 430, 445 and 430 nm, respectively, which may be assigned to splitting of d-d orbital of metal ions. The Co(II), Ni(II) and Cu(II) complexes showed band at 333, 331 and 330 nm, respectively, which may be assigned to ligand-to-metal charge transfer.

### Electronic spectra and magnetic measurements

The electronic spectra of metal complexes showed different bands at different wavelengths. The diffused reflectance spectrum of Cr(III) complex showed three bands at 28,571, 25,000 and 12,626  $\text{cm}^{-1}$ , respectively, which were assigned to the three  ${}^4A_{2g} \rightarrow {}^4T_{2g}(F)$ ,  ${}^4A_{2g} \rightarrow {}^4T_{1g}(F)$  and  ${}^4A_{2g}(F) \rightarrow {}^4T_{1g}(P)$  transitions. The magnetic susceptibility  $\mu_{\text{eff}}$  value was 4.47 BM which indicated the octahedral geometry [30, 31]. The diffused reflectance spectrum of Mn(II) complex showed three bands at 25,000, 22,727 and 15,873  $\text{cm}^{-1}$ , respectively, which correspond to  ${}^4T_{1g} \rightarrow {}^6A_{1g}$ ,  ${}^4T_{2g}(G) \rightarrow {}^6A_{1g}$  and  ${}^4T_{1g}(D) \rightarrow {}^6A_{1g}$  transitions. The complex had  $\mu_{\text{eff}}$  value 5.72 BM, which suggested an octahedral geometry [30–32]. The diffused reflectance spectrum of Fe(III) complex showed two bands at 21,978 and 17,699  $\text{cm}^{-1}$  which were assigned to  ${}^6A_{1g} \rightarrow T_{2g}(G)$ ,  ${}^6A_{1g} \rightarrow {}^5T_{1g}$  transitions. The magnetic momentum value was found to be 5.38 BM which was assigned to an octahedral geometry [31]. Co(II) complex showed three bands at 23,923, 17,035 and 15,873  $\text{cm}^{-1}$ , respectively, which were assigned to  ${}^4T_{1g} \rightarrow {}^4T_{2g}(F)$ ,  ${}^4T_{1g} \rightarrow {}^4A_{2g}(F)$  and  ${}^4T_{1g}(F) \rightarrow {}^4T_{1g}(P)$  transitions. The

spectrum also showed a band at 29,411  $\text{cm}^{-1}$  which may be attributed to ligand-to-metal charge transfer. The magnetic momentum value was found to be 5.44 BM which was assigned to an octahedral geometry [30, 31]. In Ni(II) complex, three bands at 21,594, 17,301 and 15,873  $\text{cm}^{-1}$  were shown, respectively. The bands were corresponding to  ${}^3A_{2g}(F) \rightarrow {}^3T_{1g}(P)$ ,  ${}^3A_{2g}(F) \rightarrow {}^3T_{1g}(F)$  and  ${}^3A_{2g}(F) \rightarrow {}^3T_{1g}$  transitions. The spectrum showed band at 25,000  $\text{cm}^{-1}$  that may be attributed to ligand-to-metal charge transfer. The magnetic momentum value was 3.13 BM which was assigned to an octahedral geometry [30, 31]. The diffused reflectance spectrum of Cu(II) showed two bands at 15,822 and 21,321  $\text{cm}^{-1}$  corresponding to  ${}^2E_g \rightarrow {}^2T_{2g}(D)$  and  ${}^2B_{1g} \rightarrow {}^2A_{1g}$  transitions. The spectrum showed band at 29,199  $\text{cm}^{-1}$  which may be attributed to ligand-metal charge transfer. The magnetic momentum value was 1.92 BM which was assigned to the octahedral geometry [30, 31]. The Zn(II) and Cd(II) complexes were diamagnetic and have octahedral geometry according to the suggested empirical formula listed in Table 1.

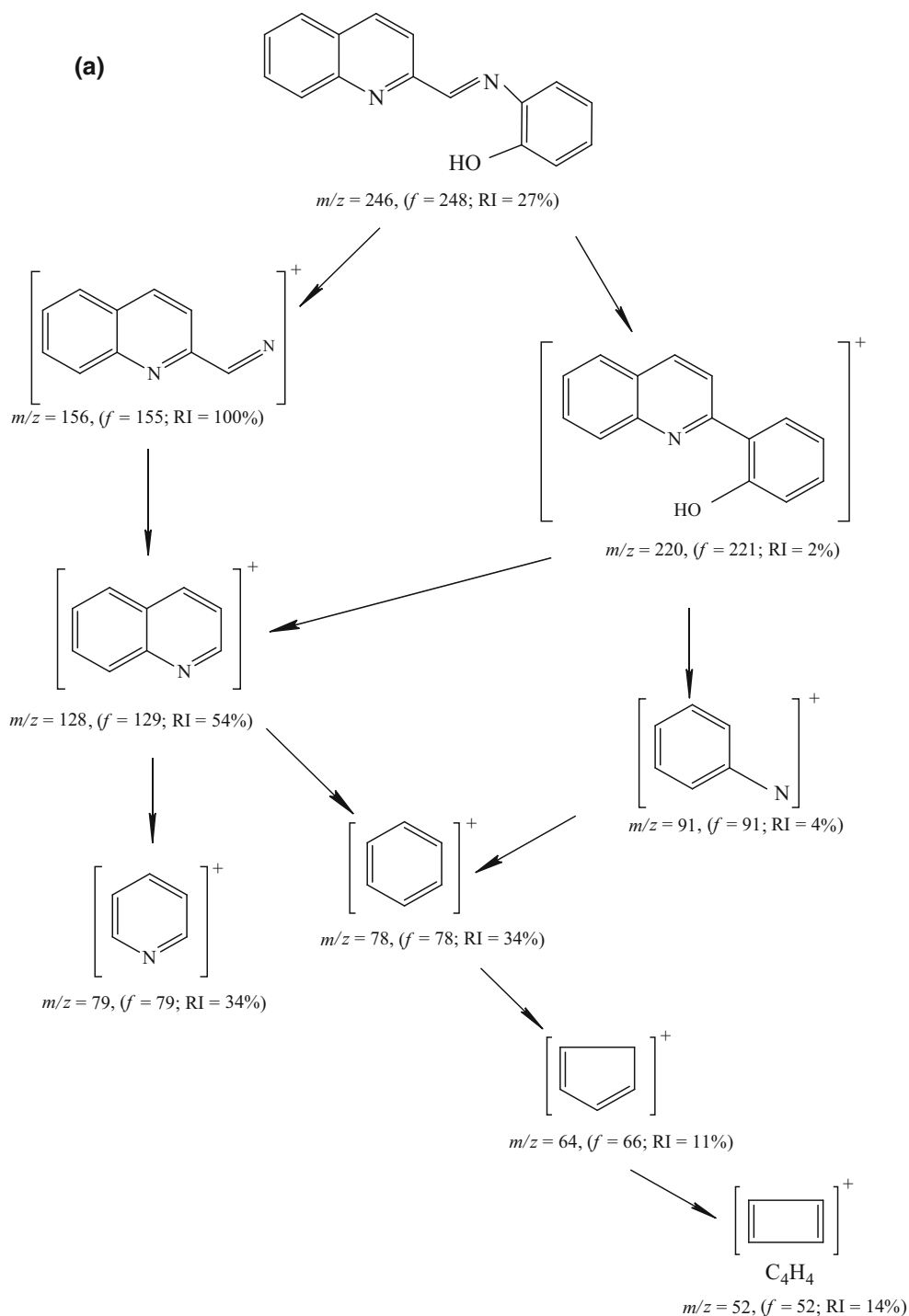
### Mass spectrum

The electron impact mass spectrum of Schiff base ligand (HL) was recorded and investigated at 70 eV of electron energy. The mass spectra of the studied Schiff base ligand (Scheme 3a) and  $[\text{Cr}(\text{L})(2,2'\text{-bipy})(\text{H}_2\text{O})]\text{Cl}_2 \cdot 2\text{H}_2\text{O}$  (Scheme 3b) complex were characterized by moderate to high relative intensity molecular ion peaks. The abundance of the molecular ion depends mainly on the structure. The molecular ion peak was found at  $m/z = 246$  amu and at  $m/z = 580$  amu for ligand and Cr(III) complex, respectively.

### IR spectra

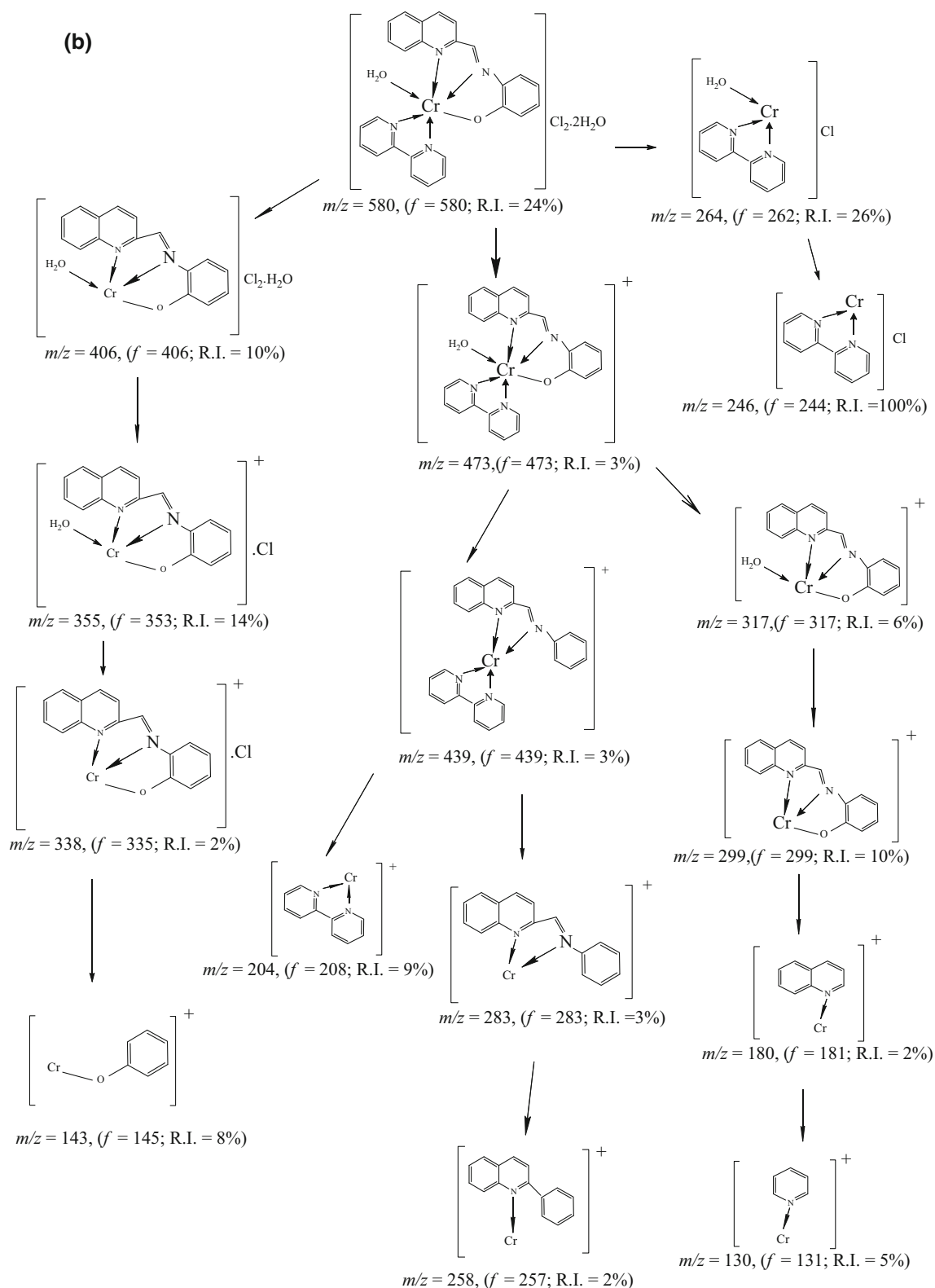
The data of the IR spectra of Schiff base ligand (HL) and the mixed ligand complexes are listed in Table 2. The IR spectra of the complexes were compared with those of the free ligand in order to determine the coordination sites that may be involved in chelation. There were some guide peaks, in the spectra of the ligand, which were of good help for achieving this goal. The position and/or the intensities of peaks were expected to be changed upon chelation. New peaks also appeared due to chelation. The IR spectra of Schiff base ligand showed strong band at 1662  $\text{cm}^{-1}$  which may be attributed to  $\nu(\text{CH}=\text{N})$  of azomethine group. The band was shifted by 5–22  $\text{cm}^{-1}$  to lower wavenumbers in most complexes or disappeared as in Cu(II) and Cd(II) complexes, indicating its involvement in the coordination [7, 32]. A broad band at 3440  $\text{cm}^{-1}$  was assigned to the presence of  $\nu(\text{OH})$  of phenolic group [7, 33]. A medium-intensity band was shown at 1282  $\text{cm}^{-1}$  which was

**Scheme 3 a** Mass fragmentation pattern of Schiff base ligand (HL). **b** Mass fragmentation pattern of  $[\text{Cr}(\text{L})(2,2'\text{-bipy})\text{H}_2\text{O}]\text{Cl}_2 \cdot 2\text{H}_2\text{O}$  complex



corresponding to the presence of phenolic  $\nu(\text{C}-\text{O})$  group. It was shifted to higher wavenumbers by  $(27\text{--}35 \text{ cm}^{-1})$  during the complexation, indicating the coordination of metal ions with deprotonated phenolic group confirmed by the disappearance of the stretching phenolic band [7]. The IR spectrum of the ligand showed a sharp and strong band at  $1592 \text{ cm}^{-1}$ , which could be attributed to the vibration  $\nu(\text{C}=\text{N})$  of the pyridyl ring [34]. The band was shifted to

higher wavenumbers  $(2\text{--}7 \text{ cm}^{-1})$  indicating the involvement of the nitrogen atom of pyridine into the coordination sphere. The in-plane bending vibration of the pyridyl ring of the ligand  $\delta(\text{C}=\text{N})$  band was observed at  $620 \text{ cm}^{-1}$  and for the complexes at  $628\text{--}658 \text{ cm}^{-1}$  which further support the coordination via pyridyl nitrogen [34]. Upon chelation of bipy, the stretching vibration of the  $\text{C}=\text{N}$  functional group of free bipy at  $1528 \text{ cm}^{-1}$  was found to be shifted to



**Scheme 3** continued

higher wavenumbers ( $1566\text{--}585\text{ cm}^{-1}$ ) [35, 36]. The characteristic out-of-plane bending modes of free bipy at  $848$  and  $656\text{ cm}^{-1}$  were shifted to lower wavenumbers

( $836\text{--}840\text{ cm}^{-1}$ ) and ( $630\text{--}653\text{ cm}^{-1}$ ) in the complexes, respectively [35, 36]. Broad absorption bands were existing in spectra of metal complexes in the region from  $3414$  to

**Table 2** Characteristic IR bands ( $\text{cm}^{-1}$ ) for Schiff base ligand (HL) and its mixed ligand complexes

Compound	$\nu(\text{H}_2\text{O})$	$\nu(\text{OH})$	$\nu(\text{CH}=\text{N})$	$\nu(\text{C}-\text{O})$	$\nu(\text{C}=\text{N})$ of bipy	$\nu(\text{C}=\text{N})/\text{pyridyl}$ ring of quinoline	$\nu(\text{M}-\text{N})$	$\nu(\text{M}-\text{O})$
HL	–	3440 b	1662 s	1282 m	–	1592 m	–	–
2,2'-Bipy	–	–	–	–	1528 w	–	–	–
$[\text{Cr}(\text{L})(2,2'\text{-bipy})(\text{H}_2\text{O})]\text{Cl}_2 \cdot 2\text{H}_2\text{O}$	3414 b/h	–	1644 s	1312 m	1566 w	1600 m	450 w	526 w
$[\text{Mn}(\text{L})(2,2'\text{-bipy})(\text{H}_2\text{O})]\text{Cl}$	3431 b/w	–	1657 w	1314 m	1580 w	1595 m	479 w	540 w
$[\text{Fe}(\text{L})(2,2'\text{-bipy})\text{Cl}]\text{Cl} \cdot 3\text{H}_2\text{O}$	3428 b/h	–	1657 h	1311 m	1579 w	1599 m	448 w	505 w
$[\text{Co}(\text{L})(2,2'\text{-bipy})(\text{H}_2\text{O})]\text{Cl}$	3427 b/w	–	1653 w	1309 m	1569 w	1597 m	447 w	522 w
$[\text{Ni}(\text{L})(2,2'\text{-bipy})(\text{H}_2\text{O})]\text{Cl} \cdot \text{H}_2\text{O}$	3426 b/h	–	1640 w	1313 w	1581 w	1598 m	425 w	520 w
$[\text{Cu}(\text{L})(2,2'\text{-bipy})(\text{H}_2\text{O})]\text{Cl} \cdot \text{H}_2\text{O}$	3431 b/m	–	Disappeared	1312 m	1575 w	1598 m	466 w	540 w
$[\text{Zn}(\text{L})(2,2'\text{-bipy})\text{Cl}] \cdot \text{H}_2\text{O}$	3430 b/w	–	1655 w	1315 m	1571 w	1599 m	412 w	530 w
$[\text{Cd}(\text{L})(2,2'\text{-bipy})\text{Cl}] \cdot 2\text{H}_2\text{O}$	3420 b/w	–	Disappeared	1317 m	1585 w	1599 m	431 w	525 w

*b* broad, *w* weak, *m* medium, *s* sharp

$3431 \text{ cm}^{-1}$  which may be assigned to stretching vibration of  $\nu(\text{OH})$  of hydrated or coordinated water molecules which were accompanied with characteristic bending band from  $833$  to  $844 \text{ cm}^{-1}$  [1, 7, 31]. New bands appeared in region  $412$ – $479$  and  $505$ – $540 \text{ cm}^{-1}$  corresponding to the metal coordination through N (M–N) and O (M–O) atoms, respectively [1, 31].

### $^1\text{H}$ NMR spectra

The  $^1\text{H}$  NMR spectrum of the free Schiff base ligand (HL) was characterized by singlet proton of azomethine ( $\text{CH}=\text{N}$ ) at  $\delta = 8.65$  ppm (s, 1H), multiple signals at  $\delta = 6.38$ – $8.13$  ppm (m, 10H) referring to the aromatic ring and quinoline and characteristic singlet signal of phenolic OH proton at  $\delta = 10.80$  ppm (s, 1H). The  $^1\text{H}$  NMR spectra of Zn(II) and Cd(II) complexes were characterized by significant down-field shifts in the peak position of azomethine ( $\text{CH}=\text{N}$ ) proton at  $\delta = 8.69$  and  $8.73$  ppm, respectively, indicating the complexation through azomethine group. The absence of phenolic proton signal supported its involvement in the chelation through proton displacement. Also, the resonance of aromatic protons had been shifted to  $6.48$ – $8.56$  and  $6.47$ – $8.70$  ppm (m, 18H), respectively, as a result of the coordination of metal ions with quinoline and (2,2'-bipy) nitrogen atoms [37]. Signals at  $\delta = 3.33$  ppm (s, 2H) and  $\delta = 3.28$  ppm (s, 4H) had been appeared, respectively, due to the presence of hydrated water in Zn(II) and Cd(II) complexes [31].

### Thermal analysis

Thermogravimetric analysis TG curve of Schiff base ligand (HL) and mixed ligand complexes is given in Table 3. The Schiff base ligand was decomposed in two steps within the

temperature range from  $150$  to  $700$  °C with total mass loss of 100% (calcd. 100%). The first step of decomposition range ( $150$ – $465$  °C) involved mass loss of 37.50% (calcd. 37.90%) which was corresponding to loss of  $\text{C}_6\text{H}_6\text{O}$  molecule. Second step of decomposition within the range of  $465$ – $700$  °C with mass loss of 62.50% (calcd. 62.09%) corresponds to the loss of  $\text{C}_{10}\text{H}_6\text{N}_2$  molecule.

Thermogravimetric analysis TG of Cr(III) complex showed its decomposition in three steps within the temperature range derived from  $30$  to  $700$  °C and a total mass loss of 78.77% (calcd. 78.49%). The first decomposition step occurred within the temperature range  $30$ – $150$  °C with mass loss of 4.66% (calcd. 4.65%) corresponding to the loss of hydrated and coordinated water molecules. Second decomposition step occurred within the temperature range ( $150$ – $400$  °C) with 17.51% (calcd. 15.52%) corresponding to the loss of  $2\text{NH}_3$  and  $2\text{HCl}$  molecules. Third decomposition step occurred within the temperature range  $400$ – $700$  °C with mass loss of 58.60% (calcd. 58.62%) corresponding to the loss of  $\text{C}_{22}\text{H}_{18}\text{N}_2\text{O}$  molecule. Finally, 21.23% (calcd. 21.51%) metallic residue remained in a form of metal oxide  $1/2(\text{Cr}_2\text{O}_3)$  residue contaminated with carbon.

Mn(II) complex showed a decomposition in two steps within the temperature range derived from  $50$  to  $700$  °C with total mass loss of 81.33% (calcd. 81.59%). The first decomposition step occurred within the temperature range  $50$ – $500$  °C with mass loss of 51.13% (calcd. 51.23%) which was corresponding to the loss of coordinated water and  $\text{C}_{14}\text{H}_{12}\text{N}_2$  molecules. Second decomposition step occurred within the temperature range  $500$ – $700$  °C with mass loss of 30.20% (calcd. 30.36%) which was corresponding to loss of HCl and  $\text{C}_{10}\text{H}_6\text{N}_2$  molecules. Finally, 18.67% (calcd. 18.41%) MnO remained as residue contaminated with carbon.

Fe(III) complex showed a decomposition in three steps within the temperature range derived from  $45$  to  $700$  °C

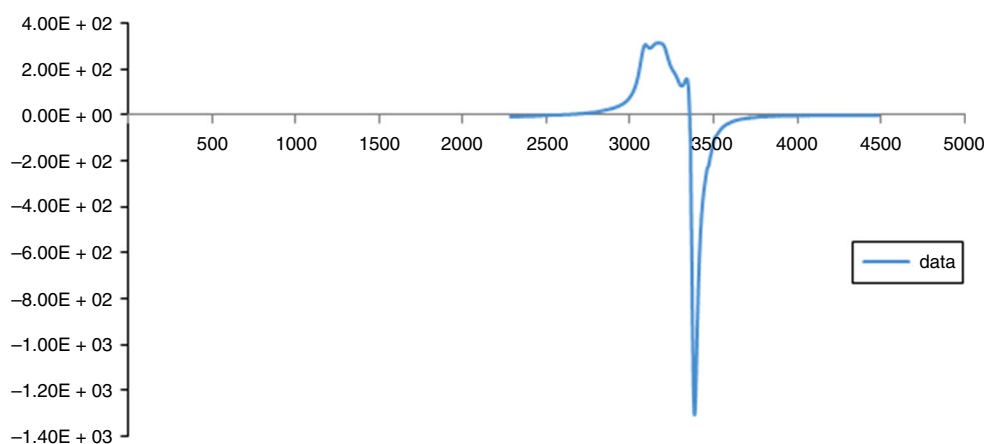


**Table 3** Thermal analysis of Schiff base ligand (HL) and mixed ligand complexes

Compound	TG rang/°C	DTG <sub>max</sub> /°C	<i>n</i> <sup>a</sup>	Mass loss% calcd./found	Total mass loss % calcd./found	Assignment	Metallic residue
HL	150–465	285	1	37.50/37.50	100/100	Loss of C <sub>6</sub> H <sub>5</sub> O	–
	465–700	610	1	62.50/62.50		Loss of C <sub>10</sub> H <sub>7</sub> N <sub>2</sub>	
[Cr(L)(2,2'-bipy)(H <sub>2</sub> O)]Cl <sub>2</sub> ·2H <sub>2</sub> O	30–150	65	1	4.66/4.65	78.71/78.78	Loss of 1/2H <sub>2</sub> O	1/2(Cr <sub>2</sub> O <sub>3</sub> ) + 4C
	150–400	300	1	15.52/15.51		Loss of NH <sub>3</sub> + 2HCl	
	400–700	565	1	58.62/58.60		Loss of C <sub>22</sub> H <sub>18</sub> N <sub>3</sub> O	
[Mn(L)(2,2'-bipy)(H <sub>2</sub> O)]Cl	50–500	410	2	51.23/51.13	81.59/81.33	Loss of H <sub>2</sub> O + C <sub>14</sub> H <sub>12</sub> N <sub>2</sub> Cl	MnO + 2C
	500–700	610	1	30.36/30.20		Loss of C <sub>10</sub> H <sub>7</sub> N <sub>2</sub>	
[Fe(L)(2,2'-bipy)Cl]Cl <sub>2</sub> ·3H <sub>2</sub> O	45–175	110	1	4.62/4.62	84.35/84.35	Loss of 1/2H <sub>2</sub> O	1/2(Fe <sub>2</sub> O <sub>3</sub> ) + C
	175–420	330	1	37.10/37.10		Loss of C <sub>9</sub> H <sub>10</sub> N <sub>2</sub> Cl <sub>2</sub>	
	420–700	490	1	42.63/42.63		Loss of C <sub>16</sub> H <sub>13</sub> N <sub>2</sub> O	
[Co(L)(2,2'-bipy)(H <sub>2</sub> O)]Cl	40–240	75	1	3.49/3.49	83.11/83.12	Loss of H <sub>2</sub> O	CoO + C
	240–495	380	1	37.14/37.15		Loss of C <sub>10</sub> H <sub>8</sub> N <sub>2</sub> Cl	
	495–800	600	1	42.48/42.48		Loss of C <sub>15</sub> H <sub>11</sub> N <sub>2</sub>	
[Ni(L)(2,2'-bipy)(H <sub>2</sub> O)]Cl <sub>2</sub> ·H <sub>2</sub> O	45–300	75/160	2	13.37/13.36	85.82/85.63	Loss of 2H <sub>2</sub> O + HCl	NiO
	300–490	380/445	2	29.13/29.50		Loss of C <sub>10</sub> H <sub>8</sub> N <sub>2</sub>	
	490–700	560	1	43.32/42.75		Loss of C <sub>16</sub> H <sub>12</sub> N <sub>2</sub>	
[Cu(L)(2,2'-bipy)(H <sub>2</sub> O)]Cl <sub>2</sub> ·H <sub>2</sub> O	35–160	100	1	6.70/6.60	81.11/80.72	Loss of 2H <sub>2</sub> O	CuO + 2C
	160–440	260	1	35.72/35.40		Loss of HCl + C <sub>10</sub> H <sub>8</sub> N <sub>2</sub>	
	440–800	650	1	38.70/38.68		Loss of C <sub>14</sub> H <sub>12</sub> N <sub>2</sub>	
[Zn(L)(2,2'-bipy)Cl] <sub>2</sub> ·H <sub>2</sub> O	70–500	360	1	40.36/39.98	84.50/84.84	Loss of H <sub>2</sub> O + HCl + C <sub>10</sub> H <sub>8</sub> N <sub>2</sub>	ZnO
	500–700	590	1	44.48/44.52		Loss of C <sub>16</sub> H <sub>12</sub> N <sub>2</sub>	
[Cd(L)(2,2'-bipy)Cl] <sub>2</sub> ·2H <sub>2</sub> O	75–425	130, 325	2	43.41/42.28	76.46/76.16	Loss of 2H <sub>2</sub> O + C <sub>15</sub> H <sub>11</sub> N <sub>2</sub>	CdO + C
	425–650	515	1	33.00/32.88		Loss of C <sub>10</sub> H <sub>10</sub> N <sub>2</sub> Cl	

<sup>a</sup> *n* number of decomposition stage

**Fig. 1** ESR spectrum of [Cu(L)(2,2'-bipy)(H<sub>2</sub>O)]Cl·H<sub>2</sub>O complex



with total mass loss 84.35% (calcd. 84.35%). The first decomposition step occurred within the temperature range 45–175 °C with mass loss of 4.62% (calcd. 4.62%) corresponding to the loss of hydrated water molecules. Second decomposition step occurred within the temperature range 175–420 °C with mass loss of 35.10% (calcd. 35.10%) corresponding to loss of 2HCl, C<sub>9</sub>H<sub>10</sub>N<sub>2</sub> molecules. Third decomposition step occurred within the temperature range 420–700 °C with mass loss of 42.63% (calcd. 42.63%) corresponding to the loss of C<sub>16</sub>H<sub>11</sub>N<sub>2</sub>O molecule. Finally, 15.81% (calcd. 15.81%) metallic residue remained as 1/2(Fe<sub>2</sub>O<sub>3</sub>) contaminated with carbon.

Co(II) complex showed a decomposition occurred in three steps within the temperature range derived from 40 to 800 °C with total mass loss of 83.89% (calcd. 83.88%). The first decomposition step occurred within the temperature range 40–240 °C with mass loss of 3.49% (calcd. 3.49%) corresponding to the loss of coordinated water molecules. Second decomposition step occurred within the temperature range 240–495 °C with mass loss of 37.15% (calcd. 37.14%) corresponding to loss of HCl and C<sub>10</sub>H<sub>8</sub>N<sub>2</sub> molecules. Third decomposition step occurred within the temperature range 495–800 °C with mass loss of 42.48% (calcd. 42.48%) corresponding to the loss of C<sub>15</sub>H<sub>10</sub>N<sub>2</sub> molecule. Finally, 16.89% (calcd. 16.88%) metallic residue remained as CoO contaminated with carbon.

Ni(II) complex showed a decomposition in three steps within the temperature range derived from 45 to 700 °C with total mass loss 85.63% (calcd. 85.82%). The first decomposition step occurred within the temperature range 45–300 °C with mass loss of 13.36% (calcd. 13.37%) which was corresponding to loss of hydrated, coordinated water and HCl molecules. Second decomposition step occurred in two stages within the temperature range 300–490 °C with mass loss 29.50% (calcd. 29.13%) which corresponding to loss of C<sub>10</sub>H<sub>8</sub>N<sub>2</sub> molecule. Third decomposition step occurred within the temperature range 490–700 °C with mass loss of 42.75% (calcd. 43.32%)

which corresponding to the loss of C<sub>16</sub>H<sub>12</sub>N<sub>2</sub> molecule. Finally, 14.37% (calcd. 14.18%) metallic residue remained as NiO.

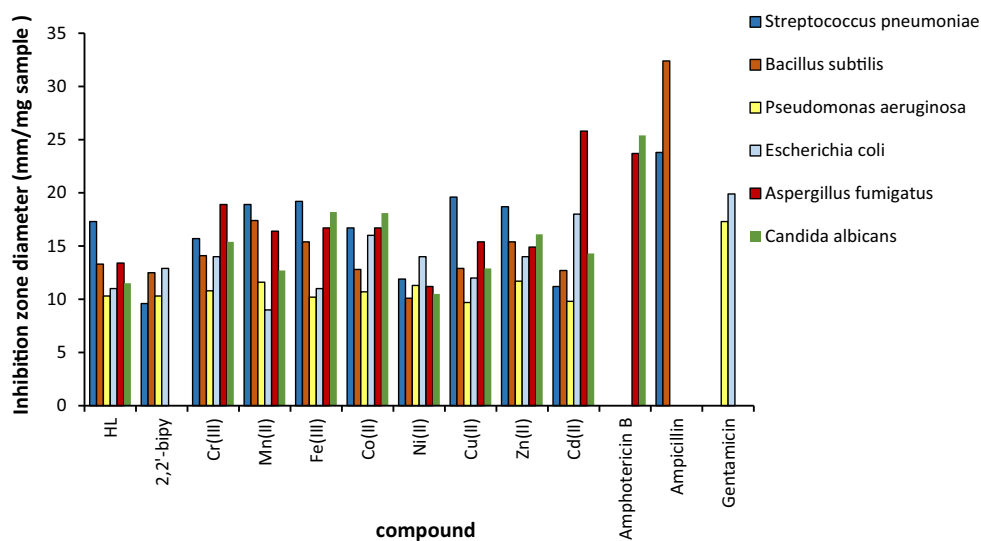
Cu(II) complex showed a decomposition in three steps within the temperature range derived from 35 to 800 °C with total mass loss of 80.72% (calcd. 80.11%). The first decomposition step occurred within the temperature range 35–160 °C with mass loss of 6.60% (calcd. 6.70%) which was corresponding to loss of hydrated and coordinated water molecules. Second decomposition step occurred within the temperature range 160–440 °C with mass loss of 35.40% (calcd. 35.72%) which was corresponding to the loss of C<sub>10</sub>H<sub>8</sub>N<sub>2</sub> and HCl molecules. Third decomposition step occurred within the temperature range 440–800 °C with mass loss of 38.68% (calcd. 38.70%) which was corresponding to the loss of C<sub>14</sub>H<sub>12</sub>N<sub>2</sub> molecule. Finally, 19.28% (calcd. 18.89%) metallic residue remained as CuO contaminated with carbon.

Zn(II) complex showed two decomposition steps which occurred within the temperature range derived from 70 to 700 °C with total mass loss 84.50% (calcd. 84.84%). The first decomposition step occurred within the temperature range 70–500 °C with mass loss of 39.98% (calcd. 40.36%) corresponding to loss of hydrated water, C<sub>10</sub>H<sub>8</sub>N<sub>2</sub> and HCl molecules. Second decomposition step occurred within the temperature range 500–700 °C with mass loss of 44.52% (calcd. 44.48%) corresponding to the loss of C<sub>16</sub>H<sub>12</sub>N<sub>2</sub> molecule. Finally, 15.59% (calcd. 15.16%) metallic residue remained as ZnO.

Cd(II) complex showed a decomposition occurred in two steps within the temperature range derived from 75 to 700 °C with total mass loss 76.16% (calcd. 76.46%). The first decomposition step occurred within the temperature range 75–425 °C with mass loss of 43.28% (calcd. 43.18%) corresponding to the loss of two hydrated water and C<sub>15</sub>H<sub>10</sub>N<sub>2</sub> molecules. Second decomposition step occurred within the temperature range 425–700 °C with mass loss of 32.88% (calcd. 33.00%) corresponding to the

**Table 4** Anti-microbial activities (antibacterial and antifungal) of Schiff base ligand (HL) and its mixed ligand complexes, the mean zone of inhibition in (mm)

Compound	Inhibition zone diameter/mm mg <sup>-1</sup>					
	Antibacterial				Antifungal	
	Gram (+)		Gram (-)		<i>Aspergillus fumigatus</i>	<i>Candida albicans</i>
	<i>Streptococcus pneumoniae</i>	<i>Bacillus subtilis</i>	<i>Pseudomonas aeruginosa</i>	<i>Escherichia coli</i>		
HL	17.3	13.3	10.3	10.9	13.4	11.5
2,2'-Bipy	9.6	12.5	10.3	12.9	NA	NA
[Cr(L)(2,2'-bipy)(H <sub>2</sub> O)]Cl <sub>2</sub> ·2H <sub>2</sub> O	15.7	14.1	10.8	11.1	18.9	15.4
[Mn(L)(2,2'-bipy)(H <sub>2</sub> O)]Cl	18.9	17.4	11.6	10.9	16.4	12.7
[Fe(L)(2,2'-bipy)Cl]Cl·3H <sub>2</sub> O	19.2	15.4	10.2	8.8	16.7	18.2
[Co(L)(2,2'-bipy)(H <sub>2</sub> O)]Cl	16.7	12.8	10.7	9.9	16.7	18.1
[Ni(L)(2,2'-bipy)(H <sub>2</sub> O)]Cl·H <sub>2</sub> O	11.9	10.1	11.3	9.9	11.2	10.5
[Cu(L)(2,2'-bipy)(H <sub>2</sub> O)]Cl·H <sub>2</sub> O	19.6	12.9	9.7	8.9	15.4	12.9
[Zn(L)(2,2'-bipy)Cl]·H <sub>2</sub> O	18.7	15.4	11.7	10.3	14.9	16.1
[Cd(L)(2,2'-bipy)Cl]·2H <sub>2</sub> O	11.2	12.7	9.8	11.3	25.8	14.3
Ampicillin	23.8	32.4	–	–	–	–
Gentamicin	–	–	17.3	19.9	–	–
Amphotericin B	–	–	–	–	23.7	25.4

**Fig. 2** Antimicrobial activity of Schiff base ligand, 2,2'-bipy and its mixed ligand complexes

loss of HCl, C<sub>10</sub>H<sub>10</sub>N<sub>2</sub> molecules. Finally, 23.84% (calcd. 23.54%) of CdO remained as residue contaminated with carbon. Thermoanalytical curves are provided as Supplementary Figure 1.

### ESR study

The solid-state ESR spectrum of Cu(II) complex exhibited axially symmetric g-tensor parameters (Fig. 1) with  $g_{\parallel} < g_{\perp} (2.06) > 2.0023$ , indicating that the copper site has a  $d_{x^2-y^2}$  ground-state characteristic of octahedral stereochemistry [1, 38]. Kivelson and Neiman [39] had reported

that  $g_{\parallel}$  value  $< 2.3$  for covalent character of the metal–ligand bond and  $> 2.3$  for ionic character.  $g_{\parallel} = 2.08$ , which indicated the covalent character of the metal–ligand bond. The trend  $g_{\parallel}(2.08) > g_{\perp}(2.06) > g_e(2.0023)$  observed for this complex showed that the unpaired electron was localized in  $d_{x^2-y^2}$  orbital of the Cu(II) ion and the spectral features were characteristics of the axial symmetry [40]. In axial symmetry, the g values were related by the expression  $G = (g_{\parallel} - 2)/(g_{\perp} - 2) = 4$ , where  $G$  is the exchange interaction parameter referring to Hathaway and Billing [41]. If the  $G$  value is greater than 4, it means that the exchange interaction between Cu(II) centers in the solid

**Fig. 3** The relation between (M–O) bond strength and inhibition zone diameter in (mm) of metal complexes

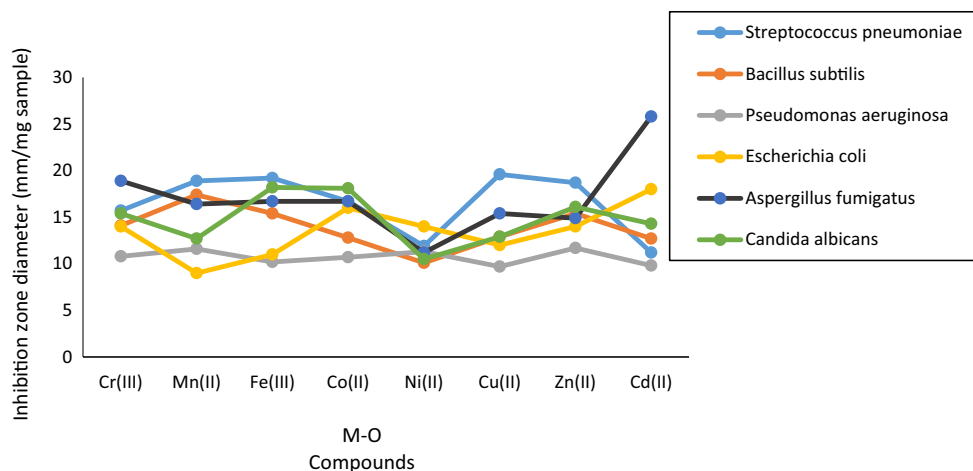
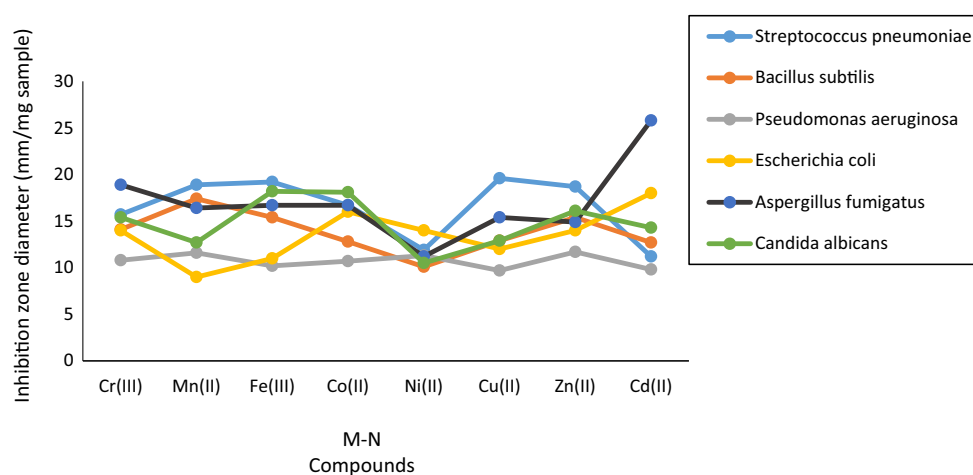


**Fig. 4** The relation between (M–N) bond strength and inhibition zone diameter in (mm) of metal complexes



state is negligible. However, when  $G$  is less than 4, this means that considerable exchange interaction will be indicated in the solid complex. The observed value for the exchange interaction parameter was  $G = 2$ , which suggested that significant exchange coupling was present.

### X-ray powder diffraction study

The XRD patterns for mixed ligand complexes showed crystalline nature; however, it showed an amorphous nature for Schiff base ligand. This might confirm that the presence of metal ions change the XRD pattern of free Schiff base ligand [42].

The average crystallite size ( $\xi$ ) can be calculated from the XRD pattern according to Debye–Scherrer equation [42, 43]:

$$\xi = \frac{K\lambda}{\beta_{1/2} \cos \theta} \quad (1)$$

where  $\lambda$  is the wavelength of X-ray radiation (1.542475 Å),  $K$  is a constant taken as 0.95 for organic compounds, and

$\beta_{1/2}$  is the width at half maximum of the reference diffraction peak measured in radians.

The dislocation density  $\delta$  indicates the number of dislocation lines per unit area of the crystal. The value of  $\delta$  is related to the average particle diameter ( $\xi$ ) from the relation [44, 45]:

$$\delta = \frac{1}{\xi^2} \quad (2)$$

The value of  $\xi$  was calculated and found to be 38.98, 53.00, 33.75, 25.62, 35.66, 30.97, 32.00 and 27.11 nm. The value of  $\delta$  was also calculated and found to be 0.00066, 0.00036, 0.00088, 0.00152, 0.00079, 0.00104, 0.00098 and 0.0014 nm<sup>-2</sup> for Cr(III), Mn(II), Fe(III), Co(II), Ni(II), Cu(II), Zn(II) and Cd(II) complexes, respectively.

### Biological activity

#### Antibacterial activity

The antimicrobial activity of Schiff base ligand (HL), 2,2'-bipy and its mixed ligand complexes is listed in Table 4

**Table 5** The screening of anticancer activity of Schiff base ligand (HL) and its mixed ligand complexes using breast cell line (MCF-7) and colon cell line (HCT-116)

Compound	(MCF-7) IC <sub>50</sub> µg	(HCT-116) IC <sub>50</sub> µg
HL	>50	22.8
[Cr(L <sup>1</sup> )(2,2'-Bipy)(H <sub>2</sub> O)]Cl <sub>2</sub> ·2H <sub>2</sub> O	39.3	22.1
[Mn(L)(2,2'-Bipy)(H <sub>2</sub> O)]Cl	28	18.8
[Fe(L)(2,2'-Bipy)Cl]Cl·3H <sub>2</sub> O	43.3	38.9
[Co(L)(2,2'-Bipy)(H <sub>2</sub> O)]Cl	24	21.5
[Ni(L)(2,2'-Bipy)(H <sub>2</sub> O)]Cl·H <sub>2</sub> O	22.7	18.2
[Cu(L)(2,2'-Bipy)(H <sub>2</sub> O)]Cl·H <sub>2</sub> O	19.9	11.9
[Zn(L)(2,2'-Bipy)Cl]·H <sub>2</sub> O	20.9	10.7
[Cd(L)(2,2'-Bipy)Cl]·2H <sub>2</sub> O	6.02	9.2

and Fig. 2. The activity against Gram-positive bacteria *Streptococcus pneumoniae* showed that Mn(II), Fe(III), Cu(II) and Zn(II) complexes have higher activity than free ligand. However, Co(II), Ni(II) and Cd(II) complexes showed lower activity than the free ligand against *Bacillus subtilis* organism. The activity against Gram-negative bacteria *Pseudomonas aeruginosa* showed that Cu(II) and Cd(II) complexes were less active than free ligand. However, Cr(III) and Cd(II) complexes showed higher activity than free ligand against *Escherichia coli*. All metal complexes recorded activity less than the standard drugs. The antimicrobial activity of complexes in relation to metal oxygen (M–O) and metal nitrogen (M–N) bond strength is shown in Figs. 3 and 4. The activity of complexes against Gram-positive bacteria was decreased as (M–O) bond strength increased, while their activity was increased as (M–N) bond strength increased. The higher activity of metal complexes could be explained on the basis of chelation. As the polarity of the metal ion has been reduced because of partial sharing of its positive charge with donor groups of the ligand and the  $\pi$ -electron delocalization on

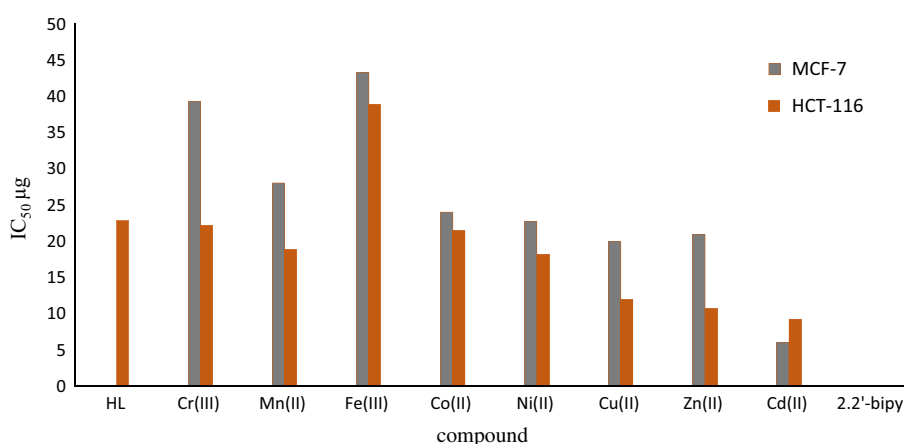
the aromatic rings, this increased the lipophilic character, favoring its permeation into the bacterial membrane and hence causing the death of the organisms [31, 46, 47].

#### Antifungal activity

The antifungal activity of Schiff base ligand, 2,2'-bipy and its complexes against *Aspergillus fumigatus* and *Candida albicans* is listed in Table 4 and presented in Fig. 2. The results showed that the activity of all metal complexes was higher than free ligands except Ni(II) complex which showed less activity than free ligands. Cd(II) complex showed activity higher than the standard. The antifungal activity of complexes in relation to metal oxygen (M–O) and metal nitrogen (M–N) bonds strength is presented in Figs. 3 and 4. The activity of complexes was decreased as (M–O) and (M–N) bond strength was increased. The results may be due to the presence of chloride ion in complexes which may enhance the antimicrobial activity due to the formation of hypochlorous acid which was decomposed to HCl acid and O<sub>2</sub>. The oxygen oxidized the cellular components and destroyed the microbes. The results may also be explained due to the combination of chlorine with membrane protein and enzyme [48, 49].

#### Anticancer activity

Screening the anticancer activity of Schiff base ligand, 2,2'-bipy and its mixed ligand complexes using breast cancer cell line (MCF-7) and colon cancer cell line (HCT-116) and the value of IC<sub>50</sub> (a minimal concentration required to inhibit 50% of cells growth) are listed in Table 5 and plotted in Fig. 5. The results against breast cancer cell line (MCF-7) showed that all metal complexes have IC<sub>50</sub> higher than free ligand. Cd(II) complex has the highest activity of complexes. The complexes could be ordered due to their activities as follows Cd(II) > Cu(II) >

**Fig. 5** Anticancer activity of Schiff base ligand, 2,2'-bipy and its mixed ligand complexes

Zn(II) > Ni(II) > Co(II) > Mn(II) > Cr(III) > Fe(III) > 2,2'-bipy. The results against colon cancer cell line (HCT-116) showed that all metal complexes have IC<sub>50</sub> higher than free ligand and complexes ordered due to their activities as follows Cd(II) > Zn(II) > Cu(II) > Ni(II) > Mn(II) > Co(II) > Cr(III) > Fe(III) > 2,2'-bipy.

## Conclusions

The following conclusions have been drawn from the elemental analysis and spectroscopic studies. New Schiff base ligand (HL) was prepared from a condensation reaction between quinoline-2-carboxaldehyde and 2-aminophenol in a molar ratio 1:1. Its mixed ligand transition metal complexes, viz. 2,2'-bipy with molar ratio 1:1:1, were also synthesized and characterized. The metal complexes showed electrolytic nature, except Zn(II) and Cd(II) complexes were nonelectrolyte. Spectroscopic studies supported the suggested structure of the complexes, whereas the metal ion coordinated through azomethine group, two pyridyl nitrogen and phenolic group. The metal complexes had octahedral geometry around the metal center. XRD studies showed that mixed ligand complexes had crystalline nature, while Schiff base ligand had an amorphous nature. The complexes showed higher antibacterial and antifungal activities than free Schiff base ligand. The Cd(II) complex showed the highest IC<sub>50</sub> against breast cancer cell line (MCF-7) and colon cancer cell line (HCT-116).

## References

- Mahmoud WH, Mahmoud NF, Mohamed GG, El-Sonbati AZ, El-Bindary AA. Synthesis, spectroscopic, thermogravimetric and antimicrobial studies of mixed ligands complexes. *J Mol Struct*. 2015;1095:15–25.
- El-Sonbati AZ, Belal AAM, El-Gharib MS, Morgan S. Supramolecular structure, mixed ligands and substituents effect on the spectral studies of oxovanadium(IV) complexes of bioinorganic and medicinal relevance. *Spectrochim Acta A*. 2012;95:627–36.
- Annaraj B, Balakrishnan C, Neelakantan MA. Synthesis, structure information, DNA/BSA binding affinity and in vitro cytotoxic studies of mixed ligand copper(II) complexes containing a phenylalanine derivative and diimine co-ligands. *J Photochem Photobiol B*. 2016;160:278–91.
- Neelaeni R, Vasantha S, Keerthana R, Sivakolunthu S, Angeline T. DNA cleavage activity of novel schiff base copper(II) complexes with sulfur containing-ligand (2-(2-methyl-thio)phenylimino)methylphenol, *N*-benzylidene-2-methylthioaniline. *Asian J Pharm Clin Res*. 2016;9:277–81.
- Kudrat-E-Zahan M, Alim Abdul M, Haque MM, Lokonuzzaman A, Sher AM, Saiidul IM. Studies on the mixed ligand complexes of Co(II), Ni(II) and Cu(II) with phthalimide and heterocyclic amines. *Int J Mater Sci Appl*. 2015;4:120–3.
- Melinmath SP, Venkatesh KB, Rekha ND, AshaIyengar T. Mononuclear mixed ligand transition metal complexes: synthesis, characterization, antioxidant and antimicrobial activity along with DNA cleavage studies. *IAJPR*. 2015;5:2503–11.
- Creaven BS, Devereux M, Foltyn A, McClean S, Rosair G, Thangella VR, Walsh M. Quinolin-2(1H)-one-triazole derived Schiff bases and their Cu(II) and Zn(II) complexes: possible new therapeutic agents. *Polyhedron*. 2010;29:813–22.
- Marcaccino S, Pepino R, Pozo MC, Basurto S, Garia-valverde M, Torroba T. One-pot synthesis of quinolin-2-(1H)-ones via tandem Ugi-Knoevenagel condensations. *Tetrahedron Lett*. 2004;45:3999–4001.
- Kulkarni NV, Hegde GS, Kurdekar GS, Budagumpi S, Sathisha MP, Revankar VK. Spectroscopy, electrochemistry and structure of 3d-transition metal complexes of thiosemicarbazones with quinoline core: evaluation of antimicrobial property. *Int J Rapid Commun*. 2010;43:235–46.
- Sudha N, Selvi G. Synthesis, characterization and biological studies on Fe(II) and Zn(II) quinoline Schiff Base complexes. *Int J Chem Tech Res*. 2015;8:367–74.
- Solomon VR, Lee H. Quinoline as a privileged scaffold in cancer drug discovery. *Curr Med Chem*. 2011;18:1488–508.
- Bentzinger G, De SW, Mullié C, Agnamey P, Dassonville-Klimpt A, Sonnet P. Asymmetric synthesis of new antimalarial aminoquinolines through Sharpless aminohydroxylation. *Tetrahedron Asymmetry*. 2016;27:1–11.
- Anantacharya R, Manjulatha K, Satyanarayan ND, Santoshkumar S, Kaviraj MY. Antiproliferative, DNA cleavage, and ADMET study of substituted 2-(1-benzofuran-2-yl) quinoline-4-carboxylic acid and its esters. *Cogent Chem*. 2016;2:2016. doi:10.1080/23312009.1158382.
- Nkoana W, Nyoni D, Chellan P, Stringer T, Taylor D, Smith PJ, Hutton AT, Smith GS. Heterometallic half-sandwich complexes containing a ferrocenyl motif: synthesis, molecular structure, electrochemistry and antiplasmodial evaluation. *J Organomet Chem*. 2014;752:67–75.
- Maddela S, Makulaa A, Maddela R. Synthesis of isatin-quinoline conjugates as possible biologically active agents. *Toxicol Environ Chem*. 2014;96:1–11.
- Muruganantham N, Sivakumar R, Anbalagan N, Gunasekaran V, Leonard JT. Synthesis, anticonvulsant and antihypertensive activities of 8-substituted quinoline derivatives. *Biol Pharm Bull*. 2004;2:1683–7.
- Shinkai H, Ito T, Ida T, Kitao Y, Yamadu H, Uchida I. 4-Aminoquinolines: novel nociceptin antagonists with analgesic activity. *J Med Chem*. 2000;43:4667–77.
- Papageorgion C, Matt AV, Joergensen J, Anderson E, Wagner K, Beerli C, Than T, Borex X, Florineth A, Rihs S, Schreier MH, Weckbecker G, Hausser C. Aromatic quinolinecarboxamides as selective, orally active antibody production inhibitors for prevention of acute xenograft rejection. *J Med Chem* 2001;44:1986–92.
- Pascual-Álvarez A, Topala T, Estevan F, Sanz F, Alzuet-Piña G. Photoinduced and self-activated nuclease activity of copper(II) complexes with *N*-(Quinolin-8-yl)quinolin-8-sulfonamide—DNA and bovine serum albumin binding. *Eur J Inorg Chem*. 2016;7:982–94.
- Mruthyunjayaswamy BHM, Vivekanand DB, Mahendra RK. Synthesis, characterization and DNA cleavage studies of some transition metal complexes derived from 5-chloro-3-phenyl-*N'*(tetrazolo[1,5-a]quinolin-4-ylmethylene)-1H-indole-2-carbohydrazide. *Res J Pharm Biol Chem Sci*. 2014;5:1057–70.
- Mistry BM, Jauhari S. Synthesis and evaluation of some quinoline Schiff bases as a corrosion inhibitor for mild steel in 1 N HCl. *Res Chem Intermed*. 2013;39:1049–68.

22. Veledo MT, Pelaez-Lorenzo C, Gonzalez R, de Frutos M, Diez-Masa JC. Protein fingerprinting of *Staphylococcus* species by capillary electrophoresis with on-capillary derivatization and laser-induced fluorescence detection. *Anal Chim Acta*. 2010;658:81–6.
23. Sarmah PP, Deb B, Borah BJ, Fuller AL, Slawin AMZ, Woollins JD, Dutta DK. Rhodium(I) carbonyl complexes of quinoline carboxaldehyde ligands and their catalytic carbonylation reaction. *J Organomet Chem*. 2010;695:2603–8.
24. Qin J, Li T, Wang B, Yang Z, Fan L. A sensor for selective detection of  $Al^{3+}$  based on quinoline Schiff-base in aqueous media. *Synth Met*. 2014;195:141–6.
25. Flaschka HA. EDTA titration. 2nd ed. New York: Pergamon Press; 1964. p. 81–6.
26. Vogel AI. Textbook of quantitative inorganic analysis. 4th ed. London: Longman; 1978.
27. West TS. Complexometry with EDTA and related reagents. 3rd ed. Pools: DBH Ltd.; 1969.
28. Scott AC. Laboratory control of antimicrobial therapy. In: Collee JG, et al., editors. *Practical medical microbiology*. 13th ed. Edinburgh: Churchill Livingstone; 1989. p. 161–81.
29. Mosmann T. Rapid colorimetric assay for cellular growth and survival: application to proliferation and cytotoxicity assays. *J Immunol Methods*. 1993;65:55–63.
30. Abd El-Halim HF, Mohamed GG, El-Dessouky MM, Mahmoud WH. Ligational behaviour of lomefloxacin drug towards Cr(III), Mn(II), Fe(III), Co(II), Ni(II), Cu(II), Zn(II), Th(IV) and UO<sub>2</sub>(VI) ions: synthesis, structural characterization and biological activity studies. *Spectrochim Acta Part A*. 2011;82:8–19.
31. Mahmoud WH, Mohamed GG, El-Dessouky MM. Synthesis, characterization and in vitro biological activity of mixed transition metal complexes of lornoxicam with 1,10-phenanthroline. *Int J Electrochem Sci*. 2014;9:415–38.
32. Mohamed GG, Soliman MH. Synthesis, spectroscopic and thermal characterization of sulphiride complexes of iron, manganese, copper, cobalt, nickel, and zinc salts. Antibacterial and antifungal activity. *Spectrochim Acta Part A*. 2010;76:341–7.
33. Wei Q, Dong J, Zhao P, Li M, Cheng F, Kong J, Li L. DNA binding, BSA interaction and SOD activity of two new nickel(II) complexes with glutamine Schiff base ligands. *J Photochem Photobiol B Biol*. 2016;161:355–67.
34. Abd El-Halim HF, Mohamed GG. Synthesis, spectroscopic studies, thermal analyses, biological activity of tridentate coordinated transition metal complexes of bi(pyridyl-2-ylmethyl)amine]ligand. *J Mol Struct*. 2015;1104:91–5.
35. Meenongwa A, Brissos RF, Soikum C, Chaveerach P, Gamez P, Trongpaniche Y, Chaveerach U. Effects of N, N-heterocyclic ligands on the in vitro cytotoxicity and DNA interactions of copper(II) chloride complexes from amidino-O-methylurea ligands. *New J Chem*. 2016;40:5861–76.
36. Reddy PR, Shilpa A. Oxidative and hydrolytic DNA cleavage by Cu(II) complexes of salicylidene tyrosine schiff base and 1,10-phenanthroline/bipyridine. *Polyhedron*. 2011;30:565–72.
37. Sheikhshoaie I, Ebrahimipour SY, Lotfi N, Mague JT, Khaleghi M. Synthesis, spectral characterization, X-ray crystal structure and antimicrobial activities of two cis dioxido-vanadium(V) complexes incorporating unsymmetrical dimalonitrile-based (NNO) Schiff base ligands. *Inorg Chim Acta*. 2016;442:151–7.
38. Soliman MH, Hindy AM, Mohamed GG. Thermal decomposition and biological activity studies of some transition metal complexes derived from mixed ligands sparfloxacin and glycine. *J Therm Anal Calorim*. 2014;115:987–1001.
39. Kivelson D, Meiman R. ESR studies on the bonding in copper complexes. *J Chem Phys*. 1961;35:149–55.
40. Chandra S, Sangeetika X. EPR, magnetic and spectral studies of copper(II) and nickel(II) complexes of schiff base macrocyclic ligand derived from thiosemicarbazide and glyoxal. *Spectrochim Acta Part A*. 2004;60:147–53.
41. Hathaway BJ, D.E. Billing DE. The electronic properties and stereochemistry of mono-nuclear complexes of cu(II) ion. *Chem Rev*. 1970;5:143–207.
42. El-Sonbati AZ, Diab MA, El-Bindary AA, Mohamed GG, Morgan SM. Thermal, spectroscopic studies and hydrogen bonding in supramolecular assembly of azo rhodanine complexes. *Inorg Chim*. 2015;430:96–107.
43. El-Ghamaz NA, El-Sonbati AZ, Diab MA, El-Bindary AA, Mohamed GG, Morgan SM. Correlation between ionic radii and of metal azodye complexes and electrical conductivity. *Spectrochim Acta A*. 2015;147:200–11.
44. Velumania S, Mathew X, Sebatain PJ, Narayandass SK, Managaraj D. Structural and optical properties of hot wall deposited CdSe thin films. *Sol Energy Mater Sol Cells*. 2003;76:347–58.
45. Sasavaraja S, Salaji DS, Bedre MD, Raghunandan D, Swamy PM, Venkataraman A. Solvo-thermal synthesis and characterization of acicular  $\alpha$ -Fe<sub>2</sub>O<sub>3</sub> nanoparticles. *Bull Mater Sci*. 2011;34:1313–7.
46. El-Sonbati AZ, El-Bindary AA, Mohamed GG, Morgan SM, Hassan WM, Elkholy AK. Geometrical structures, thermal properties and antimicrobial activity studies of azodye complexes. *J Mol Liquids*. 2016;218:16–34.
47. Abd El-Halim HF, Nour El-Dien FA, Mohamed GG, Mohamed NA. Synthesis, spectroscopic, thermal characterization and antimicrobial activity of miconazole drug and its metal complexes. *J Therm Anal Calorim*. 2012;109:883–92.
48. Pelczar MJ, Chan ECS, Krieg NR. Host–parasite interaction; nonspecific host resistance. In: *Microbiology concepts and applications*, 6th ed. New York: McGraw-Hill Inc.; 1999, p. 478–9.
49. Prescott LM, Harley JP, Klien DA. *Microbiology*, 2nd ed. Wm. C. Brown Communications, Inc.; 1993.